

The helium-rich subdwarf CPD–20°1123: a post-common envelope binary evolving onto the extended horizontal branch

Naslim N.^{1*}, S. Geier^{2†}, C. S. Jeffery^{1‡}, N. T. Behara^{1,3}, V. M. Woolf⁴ & L. Classen²

¹Armagh Observatory, College Hill, Armagh BT61 9DG

²Dr Karl Remeis-Sternwarte & ECAP, Astronomisches Institut, Friedrich-Alexander Universität Erlangen-Nürnberg, Sternwartstr. 7, D 96049 Bamberg, Germany

³Institut d’Astronomie et d’Astrophysique, Université Libre de Bruxelles, Belgium

⁴Physics Department, University of Nebraska at Omaha, Omaha, NE 68182-0266, USA

Accepted Received ; in original form

ABSTRACT

Subluminous B stars come in a variety of flavours including single stars, close and wide binaries, and pulsating and non-pulsating variables. A majority have helium-poor surfaces (helium by number $n_{\text{He}} < 1\%$), whilst a minority have extremely helium-rich surfaces ($n_{\text{He}} > 90\%$). A small number have an intermediate surface helium abundance ($\approx 10 - 30\%$), accompanied by peculiar abundances of other elements. The questions posed are i) whether these abundance peculiarities are associated with radiatively-driven and time-dependent stratification of elements within the photosphere as the star evolves from an helium-enriched progenitor to become a normal helium-poor sdB star, and ii) whether these phenomena occur only in single sdB stars or are also associated with sdB stars in binaries.

We present a fine analysis of the bright intermediate-helium sdB star CPD–20°1123 (Albus 1) which shows it to be cool, for a hot subdwarf, with $T_{\text{eff}} \approx 23\,000\text{K}$ and with a surface helium abundance $\approx 17\%$ by number. Other elements do not show extraordinary anomalies; in common with majority sdB stars, carbon and oxygen are substantially depleted, whilst nitrogen is enriched. Magnesium through sulphur appear to be depleted by ≈ 0.5 dex, but chlorine and argon are substantially enhanced.

We also present a series of radial-velocity measurements which show the star to be a close binary with an orbital period of 2.3 d, suggesting it to be a post-common-envelope system.

The discovery of an intermediate helium-rich sdB star in a close binary in addition to known and apparently single exemplars supports the view that these are very young sdB stars in which radiatively-driven stratification of the photosphere is incomplete.

Key words: star: chemically peculiar (helium) stars: evolution, stars: abundances, stars: horizontal-branch, stars: subdwarf, stars: binary

1 INTRODUCTION

Subdwarf B stars are low-mass core helium burning stars with extremely thin hydrogen envelopes. They behave as helium main-sequence stars of roughly half a solar mass. Their atmospheres are generally helium deficient; radiative levitation and gravitational settling combine to make helium sink below the hydrogen-rich surface (Heber 1986), to

deplete other light elements, and to enhance abundances of heavy elements in the photosphere (O’Toole & Heber 2006).

However, almost 10% of the total subdwarf population comprise stars with helium-rich atmospheres (Green et al. 1986; Ahmad & Jeffery 2006). They have been variously classified as sdOB, sdOC and sdOD (Green et al. 1986) stars, but more recently as He-sdB and He-sdO stars (Moehler et al. 1990; Ahmad & Jeffery 2004). Their optical spectra are characterised by strong He I (He-sdB) and He II (He-sdO) lines. The helium-rich subdwarfs (He-sd’s) may be further divided into *extremely* helium-rich stars ($\approx 95\%$ of

* E-mail: nas@arm.ac.uk

† E-mail: Stephan.Geier@sternwarte.uni-erlangen.de

‡ E-mail: csj@arm.ac.uk

He-sd's having surface helium abundances $> 80\%$ by number), and a small number of *intermediate* helium-rich stars ($\approx 5\%$ of He-sd's, having surface helium abundances $> 5\%$ and $< 80\%$ by number Naslim et al. (2010)). Whilst the extreme He-sdB stars may well be the product of double helium white dwarf mergers (Zhang & Jeffery 2012), the intermediate He-sdB stars are more difficult to explain and include stars as diverse as the prototype JL 87 (Ahmad et al. 2007), the extremely peculiar LS IV-14°116 (Naslim et al. 2011), and also UVO 0512-08 and PG 0909+276 (Edelmann 2003).

CPD-20°1123 (= Albus 1 = TYC 5940 962 1) is one of the brightest known He-sdB stars with a V magnitude 11.75 ± 0.07 (Vennes et al. 2007). This object was first reported by Gill (1896) with a photographic magnitude 10.6. Caballero & Solano (2007) suggested, it might be a hot white dwarf or possibly a hot subdwarf at a distance $d \approx 40$ pc. Vennes et al. (2007) classified it as a bright helium-rich subdwarf B star with $T_{\text{eff}} = 19800\text{K}$ and $\log g = 4.55$ using low resolution optical spectra.

This paper reports a detailed atmospheric study using a high-resolution optical spectrum which confirms CPD-20°1123 to be an *intermediate* helium-rich sdB star. It also reports a radial-velocity study which shows CPD-20°1123 to be the first such star to be also a single-lined spectroscopic binary. It will be argued that these results may have profound implications for understanding the origin of *normal* sdB stars.

2 OBSERVATIONS AND RADIAL VELOCITIES

Service-mode observations of CPD-20°1123 were made at the Australian Astronomical Telescope (AAT) with the University College London Echelle Spectrograph (UCLES) on 2010 January 14 using the 31 lines/mm grating to give a wavelength coverage of $\lambda = 3820 - 5230 \text{ \AA}$. A series of six high-resolution optical spectra were made in very poor seeing ($> 3''$) with 1 arc second slit delivering a resolution $R \simeq 45000$, and a total exposure time of 9000 s. The observations were combined, flat-fielded, sky-subtracted and wavelength calibrated. The individual orders were merged and the final spectrum was normalized.

The AAT/UCLES spectrum displays strong C II, N II, Mg II, Al III, Si II, Si III, P III, S II and S III lines, together with Ar II, Cl II and Fe III. Unlike most other He-sdB stars, the optical spectrum shows relatively strong hydrogen Balmer lines along with strong Stark-broadened He I 4471, 4922, 4388 lines. This places the star in the list of hot subdwarfs with intermediate helium abundance, alongside JL 87 (Ahmad et al. 2007) and LS IV-14°116 (Naslim et al. 2011), but the absence of He II 4686 Å suggests a much lower effective temperature. The lines due to chlorine, argon and iron-group elements have not been observed in any other He-sdB star (Naslim et al. 2010).

Fifteen medium-resolution spectra were obtained with the EMMI spectrograph ($R \simeq 3400$, $\lambda = 3880 - 4380 \text{ \AA}$) mounted at the European Southern Observatory's (ESO) New Technology Telescope (NTT) in 2008 January. Reduction was done with the ESO-MIDAS package. The radial velocities (RV) were measured by fitting a set of functions

Table 1. Radial velocities of CPD-20°1123

mid-HJD	RV [km s^{-1}]	Instrument
2454476.67364	-31.8 ± 8.0	EMMI
2454476.72033	-32.0 ± 8.0	
2454477.66701	16.3 ± 8.0	
2454477.83549	27.2 ± 8.0	
2454478.61086	15.9 ± 8.0	
2454478.66696	-4.3 ± 8.0	
2454478.75702	-15.9 ± 8.0	
2454479.64573	-39.8 ± 8.0	
2454479.65126	-26.7 ± 8.0	
2454479.70277	-21.2 ± 8.0	
2454479.70722	-44.8 ± 8.0	
2454479.71159	-31.9 ± 8.0	
2454479.76992	-37.1 ± 8.0	
2454479.73092	-26.5 ± 8.0	
2454479.78020	-34.4 ± 8.0	
<hr/>		
2455211.02431	-11.5 ± 0.6	UCLES
<hr/>		
2455499.75901	-12.1 ± 0.2	FEROS
2455501.63676	31.1 ± 0.3	
2455501.64380	31.0 ± 0.3	
2455501.65652	29.7 ± 0.3	
2455501.82339	15.4 ± 0.2	
2455501.83216	14.9 ± 0.2	

to the hydrogen Balmer and neutral helium lines using the FITSB2 routine (Napiwotzki et al. 2004). Gaussians were used to match the line cores, Lorentzians for the line wings and polynomials to match the continuum. The RV of the star was found to be variable on a timescale of days. The statistical 1σ -errors of the single measurements ranged from 5 km s^{-1} to 7 km s^{-1} . In order to derive the systematic uncertainties we calculated the standard deviation of 8 RVs from spectra taken consecutively during the last night within only $\simeq 0.13$ d assuming that the orbital period is much longer than that. This standard deviation of 8 km s^{-1} was then adopted as the uncertainty for all RVs.

Six additional high-resolution spectra have been taken with FEROS ($R \simeq 48000$, $\lambda = 3750 - 9200 \text{ \AA}$) mounted at the ESO Max-Planck-Institut Garching (MPG) 2.2m telescope in 2010 October/November.

The RVs were measured with high accuracy from sharp, unblended metal and helium lines by fitting functions with the Bamberg Spectrum Plotting and Analysis Suite SPAS (Hirsch 2009). The UCLES spectra were coadded and the RV determined in the same way. The RV measurements are given in Table 1.

3 ORBITAL SOLUTION

In order to derive the orbital solution, sine curves were fitted to the RV data points in fine steps over a range of test periods. For each period the χ^2 of the best fitting sine curve was determined. The lowest χ^2 indicates the most likely period. The orbital parameters are given in Table 2.

We performed a Monte Carlo simulation for the most likely periods. For each of the 10 000 iterations, a randomised

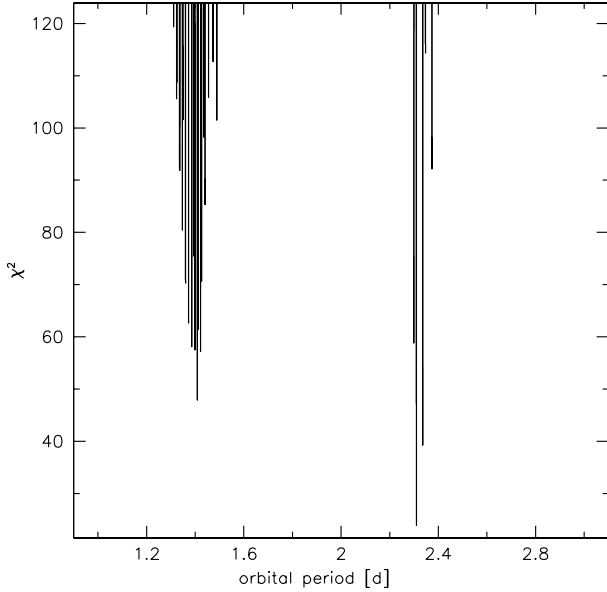


Figure 1. χ^2 of the best sine fit is plotted against the orbital period. Minima represent likely orbital periods.

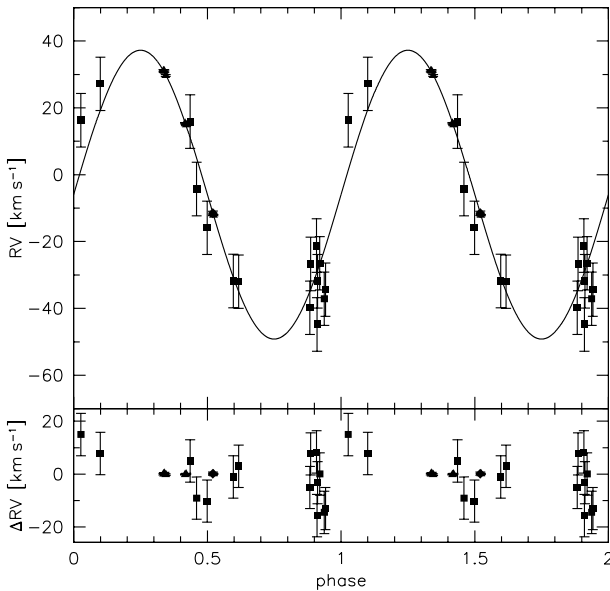


Figure 2. Radial velocities of the subdwarf plotted against orbital phase. The residuals are plotted below. Filled rectangles mark RVs measured from EMMI spectra, filled triangles mark RVs obtained from FEROS spectra and the filled diamond marks the RV measured from the coadded UCLES spectrum.

set of RVs was drawn from Gaussian distributions with central value and width corresponding to the RV measurements and the analysis repeated (see Fig. 1). The probability that the solution with the lowest χ^2 and $P = 2.3098 \pm 0.0003$ d is the correct one is estimated to be 96%. The reduced χ^2 of this solution is $\simeq 1.3$. The second best alias period

Table 2. Orbital parameters of CPD-20°1123

T_0 [HJD]	2455500.86 ± 0.01
P	2.3098 ± 0.0003 d
γ	-6.3 ± 1.2 km s $^{-1}$
K	43.5 ± 0.9 km s $^{-1}$
$f(M)$	$0.019 M_{\odot}$
M_{sdb} (adopted)	$0.47 M_{\odot}$
$M_{2,\text{min}}$	$0.21 M_{\odot}$

($P = 2.3361$ d) with $\Delta\chi^2 = 15$ has a probability of 0.8% to be the correct one (see Fig. 1).

In order to derive conservative errors for the RV semi-amplitude K and the system velocity γ we fixed the most likely period, created new RV datasets with a bootstrapping algorithm and calculated the orbital solutions. The standard deviation of these results was adopted as error estimate and is about twice as high as the 1σ -error. The phase folded RV curve is shown in Fig. 2, the orbital parameters are given in Table 2.

Adopting the frequently-assumed sdB mass of $0.47 M_{\odot}$, the minimum mass of the companion ($0.21 M_{\odot}$) can be derived from the binary mass function. No spectral features of the companion are visible. The unseen object could be a late main-sequence star with a mass ranging from $0.21 M_{\odot}$ to $\simeq 0.45 M_{\odot}$. A more massive main-sequence star would contribute sufficient light to be visible in the spectrum. The companion may also be a white dwarf. In this case its mass would be less well constrained.

Owing to the long orbital period of CPD-20°1123, it is hardly possible to detect the reflection effect due to a cool M-dwarf companion with ground-based photometry. Koen (2009) detected the reflection effect with an amplitude of 10 mmag in the sdB+M-dwarf binary JL 82. JL 82 has an orbital period of 0.75 d, making it the longest-period sdB binary in which this effect has been observed. With an orbital period three times longer, CPD-20°1123 would exhibit a reflection-effect amplitude of a few mmag at most. Whilst such signals are detectable if the periods are sufficiently short (i.e. hours), they are almost impossible to detect if the periods are of the order of days.

4 ATMOSPHERIC PARAMETERS

We measured the effective temperature T_{eff} , surface gravity $\log g$, and elemental abundances of CPD-20°1123 using the method described by Naslim et al. (2010). The microturbulent velocity determined by minimising the scatter in the nitrogen abundance was $v_t = 9 \pm 3$ km s $^{-1}$. Since, no model atmospheres with $v_t = 9$ km s $^{-1}$ were readily available, those with $v_t = 10$ km s $^{-1}$ were used in the subsequent formal solution for the ionisation equilibria and the abundance measurements. We determined T_{eff} using the ionisation equilibria of Si II/III and S II/III. The surface gravity $\log g$ was determined by using line-profile fits to the Stark-broadened He I 4471 and Balmer (H_{β} , γ , and δ) lines. The coincidence of profile fits and ionisation equilibria was used to determine the overall solution shown in Fig. 3. The ionisation equilibria and profile fits do not coincide at a single

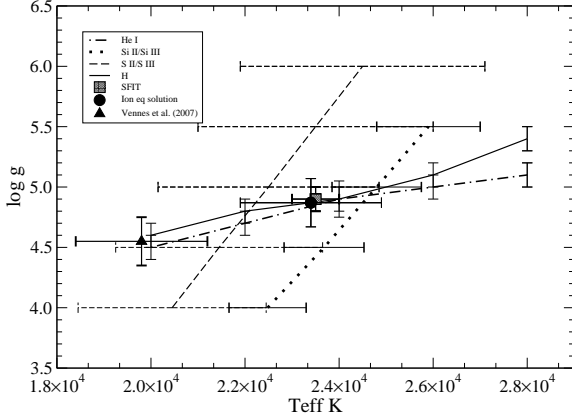


Figure 3. The loci of ionisation equilibria for Si II/III and S II/III, the profile fits to H and He I lines, and the adopted solution for CPD-20°1123.

Table 3. Atmospheric parameters of CPD-20°1123

T_{eff} (K)	$\log g$	n_{He}	Source
$23\,500 \pm 500$	4.9 ± 0.1	0.170 ± 0.05	SFIT
$23\,400 \pm 1\,500$	4.87 ± 0.2		Ion eq
$19\,800 \pm 1\,400$	4.55 ± 0.2	0.150 ± 0.15	Vennes et al. (2007)

point so that we took a weighted mean of the intersections to determine T_{eff} and $\log g$.

In addition, the χ^2 -minimization package SFIT (Ahmad & Jeffery 2003) was used to determine T_{eff} , $\log g$ and n_{He} simultaneously. Initially we selected an assumed model atmosphere grid with 1/10 solar metallicity as well as solar metallicity with $T_{\text{eff}} = 18\,000$ (2000) 28 000K, $\log g = 4.00(0.5)5.50$ and $n_{\text{He}} = 0.2, 0.3, 0.5$. We adopted a microturbulent velocity of 10 km s^{-1} . Using SFIT we obtained a reduced χ^2 fit for model with 1/10 solar metallicity and $n_{\text{He}} = 0.2$. A model atmosphere grid of $T_{\text{eff}} = 20\,000$ (2000) 26 000K, $\log g = 4.00(0.5)5.50$ and $n_{\text{He}} = 0.1, 0.2, 0.3$ was used to determine the best fit solution. The projected rotational velocity obtained from the formal solution was $v \sin i \leq 1.0 \pm 0.5 \text{ km s}^{-1}$; the true value may be slightly larger.

The atmospheric parameters of CPD-20°1123 measured using both SFIT and ionisation equilibrium agree with one another to within the formal errors and are shown in Table 3. Our estimates of T_{eff} and $\log g$ are different from the measurements by Vennes et al. (2007). The latter used an intermediate resolution optical spectrum and line-blanketed NLTE model atmospheres for their analysis. They determined T_{eff} , $\log g$ and n_{He} from the Balmer and He I lines fitting. The atmospheric parameters presented here were determined from Balmer and He I lines fitting, Si II/III and S II/III ionisation equilibria. The reason for the discrepancy might be the use of two different methods of analyses. It is noted that, Si II/III and S II/III ionisation temperatures match better the Balmer and He I lines at higher T_{eff} and $\log g$ (Fig. 3).

5 ABUNDANCES

For abundance measurements the model atmosphere with $T_{\text{eff}} = 24\,000 \text{ K}$, $\log g = 5.0$, $n_{\text{He}} = 0.2$ and 1/10 solar metallicity was adopted. After measuring the equivalent widths of all C, N, O, Mg, Al, Si, S, Cl, Ar and Fe lines using the spectrum analysis tool DIPSO, the abundances were calculated using the LTE radiative transfer code SPECTRUM (Jeffery et al. 2001). The adopted oscillator strengths (gf), equivalent widths and lines abundances are given in Table 4. Abundances are given in the form $\epsilon_i = \log n_i + c$ where $\log \sum_i a_i n_i = 12.15$ and a_i are atomic weights. This form conserves values of ϵ_i for elements whose abundances do not change, even when the mean atomic mass of the mixture changes substantially.

Mean abundances for each element are given in Table 5. The errors given in Table 5 are based on the standard deviation of the line abundances about the mean or in the case of a single representative line, the estimated error in the equivalent width measurement. Systematic shifts attributable to errors in T_{eff} and $\log g$ are given in Table 6. The line abundance for Cl II 4896.7 Å is conservatively omitted from the mean since the high abundance implied is not supported by the non-detection of Cl II 4904.7 Å.

The final best-fit spectrum using the adopted best-fit model and the elemental abundances from Table 5 is shown in Fig. 4, together with identifications for all of the absorption lines in the model. The elemental abundances shown in Table 5 are the mean abundances of all individual lines of an ion. Consequently, the cores of strong and saturated lines do not fit perfectly in Fig. 4. A few features on the observed spectrum (e.g. 4423.93 Å) are not explained by the model, but might be defects from the order merging process.

Table 5 also compares the representative range of abundances measured for normal sdB stars, for intermediate helium sdB stars JL 87 and LS IV-14°116, for extreme helium-rich sdB stars and the Sun. CPD-20°1123 appears to be metal poor ($\approx 0.5 \pm 0.3$) using magnesium, aluminium, silicon, sulphur and iron as proxies for overall metallicity. The nitrogen abundance is nearly solar and carbon is underabundant by ≈ 1.8 dex. This star shows strong argon and chlorine enrichment (≈ 0.63 and 0.9 dex, respectively). The iron group elements Sc, Ti, V, Cr and Fe have been reported in certain normal sdB stars (Geier et al. 2008, 2010; O’Toole & Heber 2006). The iron abundance in CPD-20°1123 is found to be subsolar and no detectable lines due to Sc, Ti, V and Cr were identified in the optical spectrum. The upper limit abundances of these elements were determined, assuming equivalent widths $< 5 \text{ mÅ}$ for the strongest lines of these species (Table 5). More lines due to Fe and other iron group elements should be observable in the ultraviolet. The UCLES data used for this analysis are insufficient to search for variability.

6 IS CPD-20°1123 A HELIUM-RICH STAR?

CPD-20°1123 attracted attention because it appears to be a bright sdB star with unusually strong helium lines (Vennes et al. 2007). Indeed, a fine analysis demonstrates the helium abundance to be nearly a factor of two greater than solar. This places CPD-20°1123 firmly amongst

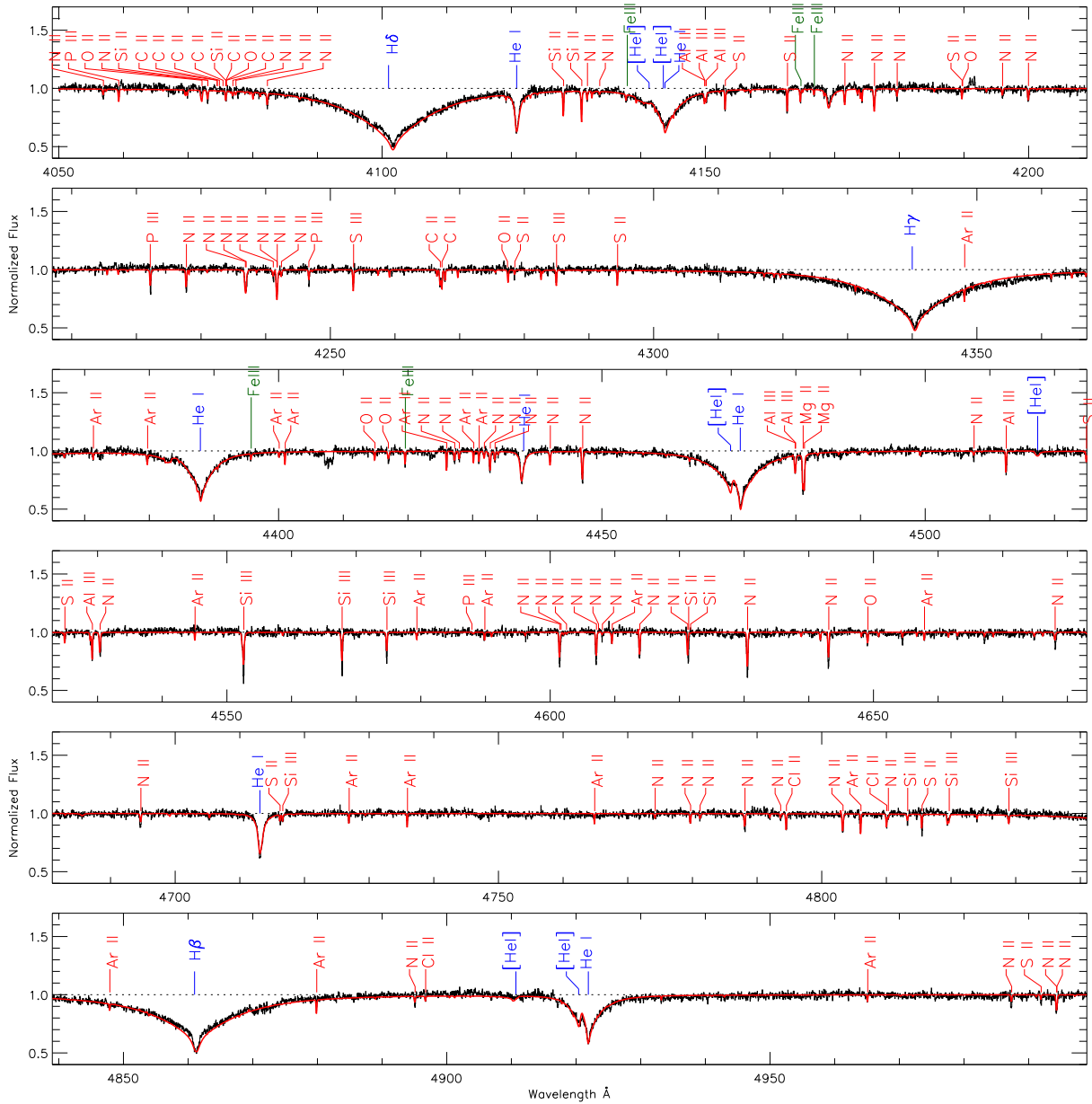


Figure 4. The merged AAT/UCLES spectrum of CPD-20°1123 along with the best FIT model of $T_{\text{eff}} = 24000\text{ K}$ and $\log g = 5.0$. Abundances are as in Table 5.

the intermediate helium-rich sdB stars alongside JL 87, LSIV-14°116, and others. A *normal* sdB star tends to have helium abundances 2 or 3 dex below solar.

The question raised by the intermediate helium-rich sdB stars is how or whether they are related to normal sdB stars, or the extreme helium-rich sdB stars, or to neither. One is tempted to distinguish the extreme helium-rich and normal sdB stars on the basis of position in the $g - T_{\text{eff}}$ diagram (Fig. 5) as well as surface composition. Zhang & Jeffery (2012) argue strongly that the former are post double-white dwarf mergers evolving onto the helium main-sequence, with surface chemistries dominated by the constituents of the merger.

The intermediate helium-rich sdB stars, on the other

hand, lie much closer to the locus of the normal sdB stars although also toward the low-gravity boundary. It is important to remember that the surface chemistry of normal sdB stars is dominated by diffusion activated by strong gradients in the radiative forces acting on different elements. The chemical separation induced by these gradients does not occur instantaneously but takes some 10^5 to 10^6 years, a small but finite fraction of the lifetime of an extended horizontal-branch star (10^8 y).

What is the surface chemistry of an sdB star progenitor? Clearly, the answer depends on what sort of star the progenitor was. Excluding double-white dwarf mergers, current understanding indicates the most likely possibilities are helium-core red giants (Dorman et al. 1993) which lose

Table 4. Individual line equivalent widths W_λ and abundances ϵ_i , with adopted oscillator strengths gf , for CPD-20°1123.

Ion	$\lambda/\text{\AA}$	$\log gf$	$W_\lambda/\text{m\AA}$	ϵ_i	Ion	$\lambda/\text{\AA}$	$\log gf$	$W_\lambda/\text{m\AA}$	ϵ_i
C II	4267.02	0.559]	58	6.71	4130.89	0.545	51	6.73	
	4267.27	0.734]			Si III	4552.62	0.283	111	6.96
N II	3995.00	0.225	116	7.89	4567.82	0.061	85	6.96	
	4041.31	0.830	80	8.07	4574.76	-0.416	60	7.17	
	4043.53	0.714	65	8.03	P III	4059.31	-0.050	22	5.62
	4236.86	0.396]	85	8.19	4222.19	0.190	40	5.74	
	4236.98	0.567]			S II	4815.52	-0.050	47	7.44
	4241.78	0.728]	72	8.19	4716.23	-0.050	22	7.50	
	4241.79	0.710]			4524.95	0.061	25	7.36	
	4447.03	0.238	75	8.08	4294.43	0.560	30	7.20	
	4601.48	-0.385	85	8.34	4162.70	0.785	33	6.97	
	4607.16	-0.483	71	8.29	4153.10	0.681	33	7.08	
	4630.54	0.093	110	8.11	S III	4253.59	0.233	36	6.72
	4056.90	-0.461	32	8.76	4284.99	-0.046	30	7.03	
	4073.05	-0.160	42	8.61	Cl II	4794.54	0.423	31	6.38
	4171.59	0.281	32	8.06	4810.06	0.281	25	6.43	
	4176.16	0.600	53	8.05	4896.74	0.450	28	6.96†	
	4530.40	0.671	51	8.12	Ar II	4401.02	-0.250	16	6.91
	4643.09	-0.385	70	8.20	4371.36	-0.570	25	7.44	
	4613.87	-0.607	70	8.41	4806.07	0.215	37	6.97	
O II	4649.14	0.342	26	7.53	4879.90	0.220	24	6.88	
	4414.90	0.210	10	7.17	4426.01	0.170	26	6.82	
	4069.88	0.365]	12	7.26	4609.60	0.286	21	7.05	
	4069.62	0.158]			4726.91	-0.180	15	7.03	
	4075.86	0.700	21	7.47	4735.93	-0.108	24	7.06	
	4416.97	-0.041	20	7.78	4764.89	-0.110	15	7.00	
Mg II	4481.13	0.568]	137	6.92	4657.90	-0.283	14	7.10	
	4481.33	0.732]			Fe III	4164.73	0.935	24	7.13
Al III	4512.54	0.405	45	6.26	4166.84	0.436	15	7.38	
	4529.20	0.660	55	6.12	4419.60	-2.218	20	7.16	
	4479.97	1.021]	43	6.44	4395.76	-2.595	12	7.30	
	4479.89	0.894]			4166.86	0.436	15	7.38	
	4149.90	0.619]	43	6.29					
	4150.14	0.464]							
Si II	4128.07	0.369	50	6.90					

gf values: C II Yan et al. (1987), N II Becker & Butler (1989), O II Becker & Butler (1988), Mg II Wiese et al. (1966) Al III Canuto, & Mendoza (1969); McEachran & Cohen (1983), Si II Becker & Butler (1990), Si III Becker & Butler (1990), P III Wiese et al. (1969), S II Wiese et al. (1969), S III Wiese et al. (1969); Hardorp & Scholz (1970), Cl II Rodriguez & Campos (1989), Ar II Wiese et al. (1969), Fe III Kurucz (1991).

†: line abundance omitted from mean in Table 5

their outer layers either by a fast stellar wind (D’Cruz et al. 1996), by stable Roche lobe overflow (Green et al. 2000), or by common-envelope ejection (Han et al. 2002). As a consequence of first dredge-up on the first giant branch, it is expected that the surface layers of the red giant will have above-solar abundances of helium and nitrogen. Since less than $0.002M_\odot$ of hydrogen-rich material survives the mass-loss episode, which is less than the natural thickness of the hydrogen-burning shell in a red giant, these remaining layers may or may not be deep enough to have been further enriched in helium. Following core-helium ignition, the surviving star contracts onto the extended-horizontal branch by one of several routes (Lanz et al. 2004;

Miller Bertolami et al. 2008, 2011) on a timescale of $\approx 10^6$ y.

Once the surface temperature exceeds some 10 000 K and the the surface gravity approaches some $10\,000\text{ cm s}^{-2}$, radiatively-driven diffusion becomes effective, and ultimately the helium and other light elements sink beneath the hydrogen. During this process, it is not inconceivable that the outer layers of the star become heavily stratified, with elements being concentrated at depths where their specific opacities are high. Such appears to be the case for the extraordinary "zirconium star" LSIV-14°116. Such exotic mixtures may simply be a precursor to that which is referred to as normal for an sdB star.

Table 5. Mean abundances ϵ_i for CPD-20°1123.

El.	CPD-20°1123	sdB ¹⁻⁵	JL 87 ⁶	LSIV-14°116 ⁷	He-sdB ⁸	Sun ⁹
H	11.85 ± 0.1	12.0	11.6	11.83	< 8.5 – 11.1	12.00
He	11.17 ± 0.1	7.9–11.0	11.3	11.15	11.5	[10.93]
C	6.71 ± 0.1	5.5–9.5	8.8	8.04	6.5–9.0	8.52
N	8.21 ± 0.21	6.5–8.5	8.8	8.02	8.0–9.0	7.92
O	7.41 ± 0.23	6.0–8.5	8.6	7.60	6.8–7.5	8.83
Ne	< 7.5	6.5–8.5	8.31	< 7.6	7.7–9.0	[8.08]
Mg	6.92 ± 0.10	5.5–7.8	7.4	6.85	7.0–8.5	7.58
Al	6.31 ± 0.13	4.5–7.0	6.3		6.0–6.4	6.47
Si	6.94 ± 0.16	5.0–7.7	7.2	6.32	6.5–7.5	7.55
P	5.68 ± 0.10	4.5–6.0	5.3			5.45
S	7.09 ± 0.28	5.0–8.0	6.9		6.0–7.0	7.33
Cl	6.40 ± 0.10					5.5
Ar	7.03 ± 0.17	6.0–9.0	6.3	< 6.5		[6.40]
Sc	< 3.5	5.0–7.0		< 5.3		3.17
Ti	< 5.8	5.3–9.0		< 6.0		5.02
V	< 6.0	6.0–8.5		< 6.5		4.00
Cr	< 6.5	5.5–8.0		< 7.0		5.67
Fe	7.27 ± 0.12	6.5–8.1	7.5	< 6.8		7.50

References: 1. Edelmann et al. (2003), 2. Geier et al. (2008), 3. Geier et al. (2010), 4. O’Toole & Heber (2006), 5. Chayer et al. (2006), 6. Ahmad et al. (2007), 7. Naslim et al. (2011), 8. Naslim et al. (2010), 9. Grevesse & Sauval (1998).

The solar helium abundance is the asteroseismic value for the outer convection zone, the solar neon and argon abundances are the meteoritic value; other solar abundances are for the solar photosphere.

Table 6. Systematic abundance errors $\delta\epsilon_i$ due to representative errors in T_{eff} and $\log g$.

Element	$\delta T_{\text{eff}} = 1000 \text{ K}$	$\delta \log g = 0.2$
C	0.05	-0.03
N	0.15	-0.06
O	0.18	-0.08
Mg	-0.09	0.03
Al	0.11	-0.05
Si	0.05	-0.04
P	0.11	-0.08
S	0.05	-0.04
Cl	-0.20	0.05
Ar	0.005	-0.02
Fe	0.11	-0.08

Now it is well-established that some 50 – 70 % (at least) of normal sdB stars are members of binary systems (Maxted et al. 2001; Geier et al. 2011). If intermediate helium-rich sdB stars are simply the precursors of normal sdB stars, then the fraction of both groups which are binaries should be the same. Until now, an argument against the precursor hypothesis was that no intermediate helium star was known to be a binary. However, such an argument only has merit with the inclusion of UVO 0512-08 and PG 0909+276 (Edelmann 2003) in addition to LSIV-14°116 (Naslim et al. 2011) and JL 87 (Ahmad et al. 2007). The discovery that CPD-20°1123 is a short-period binary with a probable white-dwarf or a late main-sequence companion reverses the argument, and supports the possibility that intermediate helium-rich and normal sdB stars derive from a similar group of progenitors. We note this is *not* the same as saying that one type evolves into the other.

Two additional facts may be important.

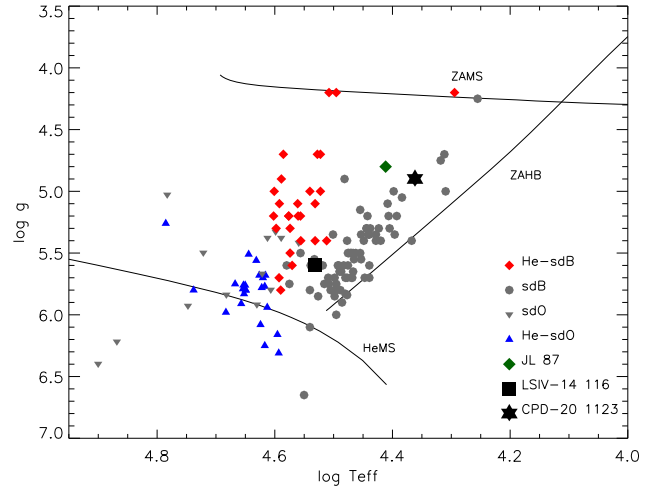


Figure 5. The location of CPD-20°1123 on the $\log g - T_{\text{eff}}$ diagram, compared with normal sdB stars (Edelmann et al. 2003) helium-rich sdB stars (Ahmad & Jeffery 2003; Naslim et al. 2010), helium-rich sdO stars (Stroeer et al. 2007), LSIV-14°116 (Naslim et al. 2011) and JL 87 (Ahmad et al. 2007). A zero-age main sequence ($Y = 0.28, Z = 0.02$), a zero-age horizontal branch ($M_c = 0.485 M_{\odot}, Y_e = 0.28, Z = 0.02$) and a helium main sequence ($Z = 0.02$) are also shown.

i) All known intermediate helium-rich sdB stars¹ have very small projected rotation velocities ($v \sin i$). A similar result has been found for normal sdB stars which are *not* in close binaries with periods less than ≈ 1.2 days (Geier et al. 2012). Slow rotation is believed to be a necessary condition

¹ JL 87, LSIV-14°116, UVO 0512-08, PG 0909+276 and CPD-20°1123

contributing to chemical peculiarity in mercury-manganese stars (Wolff & Preston 1978). Fast rotation may cause mixing effects which prevent elements from being concentrated in stratified layers.

ii) CPD-20°1123 lies at the cool end of the sdB domain. The diffusion time-scale should be longer at lower T_{eff} and g , so that peculiar surface chemistries may be relatively more likely. It would be interesting to look for more helium-strong sdB stars at the cool end of the sdB sequence.

7 CONCLUSION

With a helium abundance about twice solar, CPD -20°1123 is securely determined to be an intermediate helium-rich subdwarf B star. Chemically these are quite distinct from normal sdB stars (which are helium poor) and extremely helium-rich sdB stars (more than 80% helium). The abundances of other elements in CPD -20°1123 are slightly peculiar; high argon and chlorine, and detectable iron are noted in particular.

CPD -20°1123 is the first intermediate helium-rich sdB star found to be a short-period binary. With a period of 2.3d, the companion could be either a low-mass main-sequence star or a white dwarf.

It is argued that a high helium abundance would be expected for the surface of a very young sdB star, evolving from the tip of the first red-giant branch after having lost its hydrogen-rich envelope. This helium will sink out of sight within the first 10^6 years of evolution on the extended horizontal branch. It is proposed that the intermediate helium sdB stars are simply very young normal sdB stars in which this process has yet to be completed.

It is expected that as the number of known intermediate-helium sdB stars increases, the number found to be members of binaries will also increase, as will the variety of their surface chemistries. Understanding how the surface chemistries of these stars change is a challenge for both theory and observation but will ultimately help to explain how sdB stars are formed.

ACKNOWLEDGMENTS

This paper is based on observations obtained with the Australian Astronomical Telescope and on observations at the La Silla Observatory of the European Southern Observatory for programmes number 080.D-0685(A) and 086.D-0714(A).

The Armagh Observatory is funded by direct grant from the Northern Ireland Dept of Culture Arts and Leisure. S. G. is supported by the Deutsche Forschungsgemeinschaft under grant HE1356/49-1.

REFERENCES

Ahmad A., Behara N. T., Jeffery C. S., Sahin T., Woolf V. M., 2007, *A&A*, 465, 541
 Ahmad A., Jeffery C. S., 2003, *A&A*, 402, 335
 Ahmad A., Jeffery C. S., 2004, *Ap&SS*, 291, 233
 Ahmad A., Jeffery C. S., 2006, *Baltic Astronomy*, 15, 139
 Becker S. R., Butler K., 1988, *A&A*, 209, 244
 Becker S. R., Butler K., 1989, *A&A*, 235, 326

Becker S. R., Butler K., 1990, *A&A*, 201, 232
 Caballero J. A., Solano E., 2007, *ApJ*, 665, L151
 Canuto, W., Mendoza C., 1969, *Mexicana Astron. Astrofis*, 23, 107
 Chayer P., Fontaine M., Fontaine G., Wesemael F., Dupuis J., 2006, *Baltic Astronomy*, 15, 131
 D’Cruz N. L., Dorman B., Rood R. T., O’Connell R. W., 1996, *ApJ*, 466, 359
 Dorman B., Rood R. T., O’Connell R. W., 1993, *ApJ*, 419, 596
 Edelmann H., 2003, PhD thesis, Friedrich-Alexander-Universität Erlangen-Nürnberg
 Edelmann H., Heber U., Hagen H., Lemke M., Dreizler S., Napiwotzki R., Engels D., 2003, *A&A*, 400, 939
 Geier S., Edelmann H., Napiwotzki R., Morales-Rueda L., 2012, in *Fifth meeting on hot subdwarf stars and related objects* Vol. 452 of *Astronomical Society of the Pacific Conference Series*, Rotational properties of single and wide binary subdwarf B stars. p. 81
 Geier S., Heber U., Edelmann H., Morales-Rueda L., Napiwotzki R., 2010, *Ap&SS*, p. 329
 Geier S., Heber U., Napiwotzki R., 2008, in U. Heber, C. S. Jeffery, & R. Napiwotzki ed., *Hot Subdwarf Stars and Related Objects* Vol. 392 of *Astronomical Society of the Pacific Conference Series*, Metal Abundances of Subdwarf B Stars from SPY – a Pattern Emerges. p. 159
 Geier S., Hirsch H., Tillich A., Maxted P. F. L., Bentley S. J., Østensen R. H., Heber U., Gänsicke B. T., Marsh T. R., Napiwotzki R., Barlow B. N., O’Toole S. J., 2011, *aap*, 530, A28
 Gill D. and Kapteyn J. C., 1896, *Annals of the Cape Observatory*, 3, 1
 Green E. M., Liebert J., Saffer R. A., 2000, in *American Astronomical Society Meeting Abstracts* Vol. 32 of *Bulletin of the American Astronomical Society*, On the Origin of Subdwarf B Stars and Related Metal-Rich Binaries. p. 1477
 Green R. F., Schmidt M., Liebert J., 1986, *ApJS*, 61, 305
 Grevesse N., Sauval A. J., 1998, *Space Science Reviews*, 85, 161
 Han Z., Podsiadlowski P., Maxted P. F. L., Marsh T. R., Ivanova N., 2002, *MNRAS*, 336, 449
 Hardorp J., Scholz M., 1970, *ApJS*, 19, 193
 Heber U., 1986, *A&A*, 155, 33
 Hirsch H., 2009, PhD thesis, Universität Erlangen-Nürnberg
 Jeffery C. S., Woolf V. M., Pollacco D. L., 2001, *A&A*, 376, 497
 Koen C., 2009, *MNRAS*, 395, 979
 Kurucz R. L., 1991, in A. G. D. Philip, A. R. Upgren, & K. A. Janes ed., *Precision Photometry: Astrophysics of the Galaxy New Lines, New Models, New Colors*. p. 27
 Lanz T., Brown T. M., Sweigart A. V., Hubeny I., Landsman W. B., 2004, *ApJ*, 602, 342
 Maxted P. f. L., Heber U., Marsh T. R., North R. C., 2001, *MNRAS*, 326, 1391
 McEachran R., Cohen M., 1983, *J.Phys.B*, 16, 3125
 Miller Bertolami M. M., Althaus L. G., Unglaub K., Weiss A., 2008, *A&A*, 491, 253
 Miller Bertolami M. M., Córscico A. H., Althaus L. G., 2011, *ApJ*, 741, L3
 Moehler S., Richtler T., de Boer K. S., Dettmar R. J.,

- Heber U., 1990, *A&AS*, 86, 53
- Napiwotzki R., Yungelson L., Nelemans G., Marsh T. R., Leibundgut B., Renzini R., Homeier D., Koester D., Moehler S., Christlieb N., Reimers D., Drechsel H., Heber U., Karl C., Pauli E.-M., 2004, in R. W. Hilditch, H. Hensberge, & K. Pavlovski ed., *Spectroscopically and Spatially Resolving the Components of the Close Binary Stars* Vol. 318 of *Astronomical Society of the Pacific Conference Series*, Double degenerates and progenitors of supernovae type Ia. pp 402–410
- Naslim N., Jeffery C. S., Ahmad A., Behara N. T., Şahin T., 2010, *MNRAS*, 409, 582
- Naslim N., Jeffery C. S., Behara N. T., Hibbert A., 2011, *MNRAS*, 412, 363
- O’Toole S. J., Heber U., 2006, *A&A*, 452, 579
- Rodriguez L. F., Campos J., 1989, *J.Quant.Spectrosc.Radiat.Transfer*, 41, 377
- Stroeer A., Heber U., Lisker T., Napiwotzki R., Dreizler S., Christlieb N., Reimers D., 2007, *A&A*, 462, 269
- Vennes S., Kawka A., Smith J. A., 2007, *ApJ*, 668, L59
- Wiese W., Smith M., Glennon 1966, *National Bureau of Standards (USA) Publs*, I-II
- Wiese W., Smith M., Miles B., 1969, *National Bureau of Standards (USA) Publs*
- Wolff S. C., Preston G. W., 1978, *ApJS*, 37, 371
- Yan C., Taylor K., Seaton M., 1987, *J.Phys.B*, 20, 6399
- Zhang X., Jeffery C. S., 2012, *MNRAS*, 419, 452